J. C. Trinder
University of New South Wales
Sydney, Australia

The Effects of Photographic Noise on Pointing Precision, Detection, and Recognition

As optical magnification is increased the signal-to-noise ratio will decrease and, therefore, noise will have a greater effect on the pointing precision of observations.

Abstract: *Methods of formulating photographic granularity are summarized and a review is given on recent research into graininess, the subjective impression of granularity. It is deduced that the signal-to-noise ratio (SNR) should be formulated by the ratio of density difference of the object being viewed and the root mean square granularity measured with a scanning aperture equivalent to 48 μm at 12× optical magnification. Precisions of pointing to circular targets subject to noise are expressed in terms of this SNR. The effects on pointing observations of varying the optical magnification are also considered. Detection and recognition of geometric objects in the presence of noise vary directly with SNR and indirectly with the target size. Angular objects are more easily detected and recognized than circular objects.*

Introduction

The effects of image quality and noise on the ability of observers to perform visual tasks on displayed images are currently being researched in more detail, as image data of varying qualities derived from such sources as satellite and raster scan systems, side looking radar, and small scale photography become available. Visual performance is strongly dependent on the particular task presented to an observer. It is, therefore, necessary that it be studied under a range of variables which are relevant to particular photogrammetric and remote sensing tasks, for example, pointing observations to photogrammetric targets, or the identification of photographic features for topographic or thematic mapping. Image quality parameters such as *resolution* and *modulation transfer functions* (MTF) have not always provided users of displayed image data with sufficient information to directly relate image quality to the efficiency of given visual tasks. It has been claimed that, for remote sensing purposes, a new figure of merit is required which is more specific to the needs of remote sensing. The development of a new image quality parameter, however, should be avoided because adequate parameters are available, provided suitable research is carried out to relate these parameters to appropriate visual tasks.

In this paper the effects of noise on monocular photogrammetric pointing observations and the detection and recognition of displayed images will be studied. While the visual tasks studied are photogrammetric, the approach adopted in this research should be applicable to other tasks such as those associated with remote sensing. The methods of describing photographic granularity are summarized, expressions for the signal-to-noise ratio of targets are discussed, and results of observations to targets subject to different levels of image noise are presented. Finally, the most appropriate parameters of the target for relating results for each visual task to the signal-to-noise ratio are discussed.

Photogrammetric Engineering and Remote Sensing,
0099-1112/82/4810-1563$02.25/0

Photographic Granularity and Graininess

Trinder (1980) studied the granularity of aerial photographic emulsions using parameters shown in Figure 1: *RMS granularity* (σ_D, the root-mean-square variation in density readings); and the *Wiener Spectrum* $\Phi(u)$ (or $\Phi(u,v)$ in two dimensions) which is the Fourier transform of the correlogram $\phi(t)$ (and $\phi(t,r)$), being the correlation between n density readings $D(x_i)$ and $D(x_i + t)$ of points separated by a small distance t, Equation 1.

$$\phi(t) = \frac{1}{n} [D(x_i) - \bar{D}) (D(x_i + t) - \bar{D})] \quad (1)$$

where $\bar{D}$ is the mean density of the sample. In these expressions of film granularity, no estimate was made of the observer's subjective impression of the grain, commonly known as *graininess*. Studies by Stultz and Zweig (1959) compared samples subject to different levels of granularity to determine an optimum scanning aperture of the visual system for viewing grainy images. Zwick (1965) observed that graininess was most objectionable for diffuse densities of 0.64 for black-and-white photography, while for color photography the critical density was 0.9. Such densities are common in aerial photography. Zwick and Brothers (1975) found that the just noticeable difference (JND) in granularity depended on the type of scene viewed. For a uniform scene, the JND in granularity was 6 percent of the average density, while for "busy" scenes it rose to as high as 30 percent.

Relating these results to photogrammetric tasks is difficult because in most cases the tasks studied by these researchers are dissimilar to those associated with photogrammetry and remote sensing. Aerial photography would be described as "busy," but a conclusion that granularity has little or no influence on photogrammetry and remote sensing tasks would be premature without adequate analysis of its effects on particular visual tasks at different optical magnifications.

To pursue this study, it is necessary to determine a mathematical expression for the signal-to-noise ratio (SNR) in the photographic image.

Signal-To-Noise Ratio of Photographic Images

Ratio of Density of Target and RMS Granularity

As demonstrated in Figure 1, the RMS granularity and correlogram are dependent on the aperture used to scan the photographic sample, either circular or narrow rectangular apertures being normal. For a complete estimate of the Wiener spectrum of granularity, a narrow slit should be used while, if the granularity is to be determined for reference to visual observations, a circular aperture of appropriate size must be employed because the eye scans the sample with a circular aperture.

The Kodak standard measurement of RMS granularity uses a 48-μm diameter circular scanning aperture which is claimed to be equivalent to the scanning aperture of the eye for observation at 12× optical magnification. The 48-μm diameter aperture (equal to 9.5 μm on the retina) was derived in the tests of Stultz and Zweig (1959) because the variation in comparative judgements of the samples was smallest for this aperture. Stultz and Zweig also proved that there is an inverse linear relationship between optical magnification and the diameter of the scanning aperture of an observer's eye projected onto the image; that is, as the magnification increases the effective scanning aperture diameter of the eye decreases proportionally. Scanning apertures used by Zwick and Brothers (1975) for optical magnifications of 3× to 12×, ranged from 200 μm to 48 μm in diameter, respectively, while Charman and Olin (1965), Hufnagel (1965), Scott (1968), and Hempenius (1964) adopted scanning apertures of 24 μm in diameter for their studies. Hempenius, who studied the modulation sensitivity of the eye for repetitive sine-wave targets, stated that the scanning aperture may vary according to the particular task presented to the observer.

The work of Stultz and Zweig provides the best estimate of the scanning aperture used by the eye, if indeed a constant size of aperture does exist. For this study granularity measurements have been derived using an aperture equivalent to 48 μm in diameter at 12× magnification (i.e., 96 μm at 6× magnification). The formulation for the SNR adopted is, therefore,

$$\text{SNR} = \Delta D / \text{RMS}_{48\ \mu\text{m}} \quad (2)$$

where ΔD is the density difference of the sample above the background, and

$\text{RMS}_{48\ \mu\text{m}}$ is the root-mean-square variation in density measured with a scanning aperture equivalent to 48 μm at 12× magnification.

Typical SNR's derived for targets on aerial photography viewed at different magnifications are given later in this paper.

SNR in Frequency Domain

A SNR expressed in terms of density or luminance levels has the advantage of simplicity but lacks the additional information that is available through the use of the signal power and Wiener spectrum of noise, both of which are expressed in the spatial frequency domain as a function of lines/mm. Barnard (1972) used the ratio of signal and noise power (Wiener spectrum) to relate visual observations of detection and recognition of

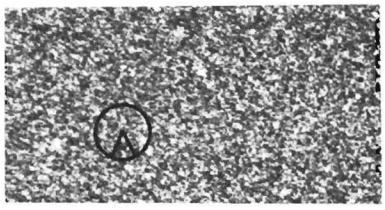

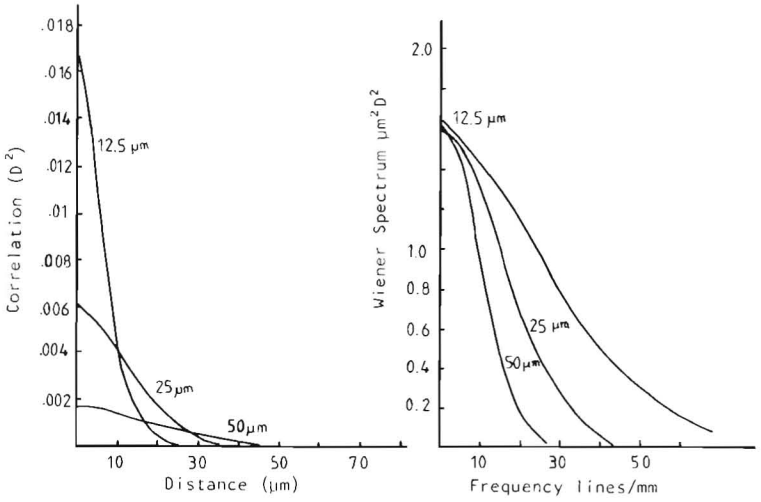

FIG. 1. The measurement of RMS granularity by recording density variations across a sample using a circular aperture. Typical correlogram for aerial film derived by Equation 1, and the Wiener Spectrum of the noise derived for different aperture diameters are shown.

geometric objects to the quality of the image. He presented a hypothesis that the eye performs as a "perfect matched filter" whereby the SNR is maximized when detecting orthogonal signals in noise. Barnard defines an orthogonal signal as one for which the signals required for detection have no common area. Hufnagel (1965) presented several formulas to relate the subjective ranking of photographic prints to parameters of image quality, each formula being composed of elements of the signal and noise power. The effect of the visual system was described by its MTF adjusted for the preferred optical magnification of the observation. Halmshaw (1971), studying x-ray films, used a similar mathematical formulation for a film quality index while James (1977), summarizing the work of a number of researchers, proposed a complex formula for SNR also based on similar components. Such multi-component formulas for SNR have not been completely tested, but appear to agree with experimental data on visual tasks. A highly analytical approach such as this is not justified for applications to photogrammetric measurements, but reference is made to the frequency domain in this paper in an attempt to understand the visual processes in more detail.

The RMS granularity and the Wiener spectrum for the two-dimensional case are mathematically related through the Fourier transform of the correlogram ($\phi(t,r)$, Equation 1) as follows:

- Wiener Spectrum $\Phi(u,v)$ = Fourier transform of $\phi(t,r)$, in units of (linear dimension)^2 · (density)^2;
- Since $\Phi(u,v)$ and $\phi(t,r)$ are transform pairs, the maximum ordinate of $\phi(t,r)$ equals the volume under $\Phi(u,v)$;
- That is, $\phi(0,0) = (\text{RMS})^2 = \int_{\infty}^{\infty}\int_{\infty}^{\infty} \Phi(u,v)du\,dv.$ (3)

By definition, $\phi(0,0)$ is equal to the $(\text{RMS})^2$ in units of $(\text{Density})^2$, which also equals the total noise power. The ratio in Equation 2 therefore includes the component of (total noise power)$^{1/2}$.

Targets observed in this study are circular sharp targets of low and medium contrast, defined by the approximately linear Equations 4.

$$f_T(x,y) = 0.4343 \cdot \frac{\Delta I}{I} \text{ for } (x^2 + y^2)^{1/2} \leq a$$
$$= 0 \qquad \text{for } (x^2 + y^2)^{1/2} > a \tag{4}$$

where x,y are rectangular coordinates of the target,

$\Delta I/I$ is the object contrast in intensity units,

a is the radius of the circular target, and

$f_T(x,y)$ is the intensity of the target with respect to its background expressed in units of density.

The power spectrum of the circular target is defined by

$$\text{Power spectrum of } f_T(x,y) = |F_T(u,v)|^2 \tag{5}$$

where $F_T(u,v)$ is the Fourier transform of $f_T(x,y)$.

Based on known relationships between Fourier transform pairs $f_T(x,y)$ and $F_T(u,v)$, units of the power spectrum given by Equation 5 will be (linear dimension)^4·(density)^2 and, therfore, cannot be related directly with the noise power. In order to obtain power spectrum units which are consistent with the units of noise power, i.e., (linear dimension)^2·(density)^2, the power spectrum of the target has been derived by taking the Fourier transform of the autocorrelation function $\phi_T(t,r)$ of the circular target scaled to a maximum value of ΔD^2, as shown in Figure 2. Graphs of power spectra of circular targets observed in this paper are shown in Figure 3. The total signal power, as shown above for the Wiener spectrum, equals $\phi_T(0,0)$ and hence is equivalent to ΔD^2.

Therefore, the expression for the SNR in Equation 2 can be rewritten as follows:

$$\text{SNR} = \frac{\Delta D}{\text{RMS}_{48\ \mu m}} = \left(\frac{\text{total signal power}}{\text{total noise power}}\right)^{1/2} \tag{6}$$

The additional parameters of maximum power and the frequency range of the targets and noise will be discussed later.

Pointing Observations

Method

The aim of this research was to analyze the effects of image noise on monocular pointing observations in the x- and y-directions (independently of the effects of other image quality parameters). Previous extensive pointing observations (Trinder, 1971) have been made on targets subject to image blur without noise; the two factors of noise and blur will be combined in a later study. For this study, different levels of image noise could be created either by observing standard photographic images under a range of optical magnifications, or by printing different levels of noise onto target images, and viewing the targets under fixed magnification. The second alternative was adopted because it allowed flexibility in the choice of both target size and noise levels and in addition was less affected by the optical quality of the observation equipment.

Noisy images were produced by double exposure of grain and targets. The grain was derived by magnification of a constant density sample of a high granularity photographic film, while the targets were obtained by printing onto the same photographic material, circular black dots reduced 4×. Background of the resulting images was made as nearly as possible equal to either 0.3D or 0.7D. A set of noiseless images was also printed for use as a standard set. Granularity of the noisy targets was measured on the Joyce Loebl microden-

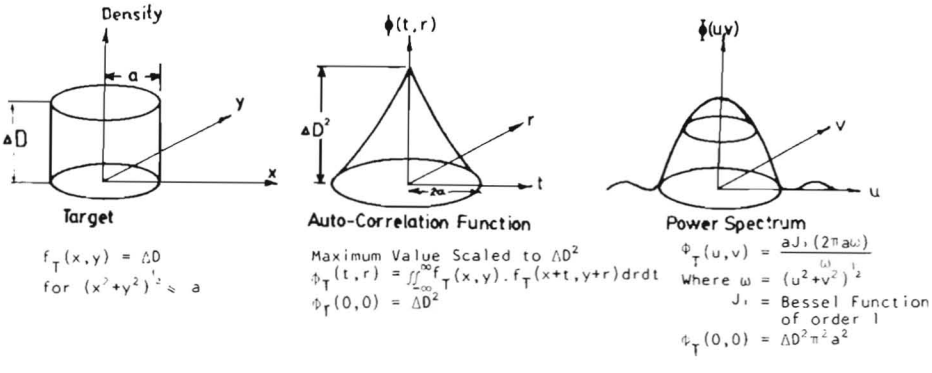

FIG. 2. Procedure for computing power spectrum of circular target. The autocorrelation function has been scaled to a value of ΔD^2 prior to the computation of the power spectrum by Fourier transform.

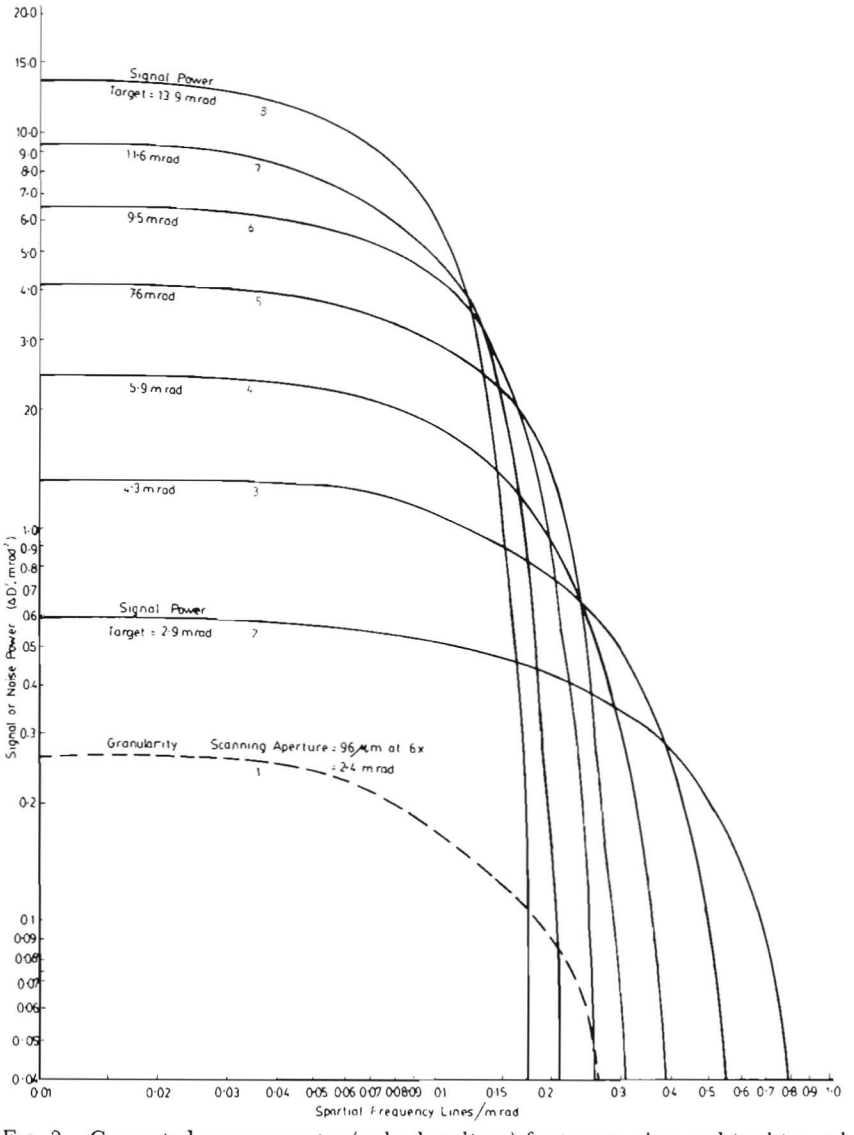

FIG. 3. Computed power spectra (unbroken lines) for targets observed in this study. Sizes are expressed in mrad, but a conversion to linear dimensions for a viewing magnification of 6× can be obtained in Figure 6. Noise power derived for one example of granularity is shown by a broken line.

sitometer using aperture diameters varying from 192 μm to 48 μm to determine the relationship between aperture and RMS.

Six targets each of seven different sizes ranging in diameter from 118 μm to 576 μm, sizes which would commonly occur in aerial surveys, were printed on the samples shown typically in Figure 4. Monocular pointing observations were performed on a Wild A8 stereoplotter at 6× optical magnification with a measuring mark of 60 μm. The left photo carrier was set to zero tilts based on measurements on a grid plate, while the scale of the model space coordinates, being 3.5× image scale, was calibrated against grid dimensions. Standard errors of observation for noiseless targets approached the least count of the machine coordinates. All linear measurements were converted to angular subtense in μrad or mrad (1 sec = 5 μrad; 1 min arc = 0.3 mrad or 12.5 μm at 6× optical magnification) by the formula

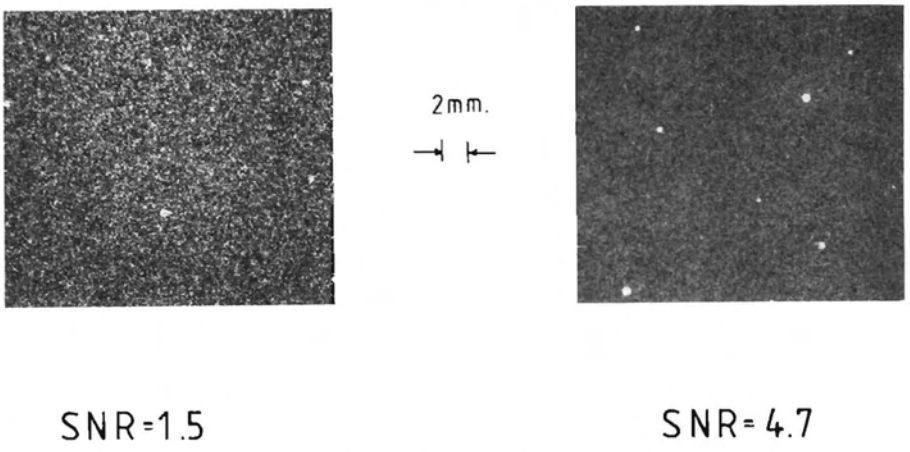

FIG. 4. Examples of noisy targets observed in this study. Dimensions and SNR of the original samples are shown. Measurements were made on these samples at an optical magnification of 6×.

$$\text{Angular Subtense (mrad)} = \frac{\text{linear dimension } (\mu\text{m}) \times \text{magnification}}{250} \quad (7)$$

where 250 mm is the observation distance for comfortable viewing. The conversion from mrad to linear dimension at 6× magnification is provided by separate axes for each set of units in all figures where results are presented.

The annulus width between the edge of the target and measuring mark when centrally placed has been established in past research as the most significant parameter of the target dimension affecting pointing precisions. Angular subtense of target sizes and corresponding target annuli are given in the table in Figure 6. Target annulus is derived from (target size—measuring mark size)/2.

Coordinates were observed on a selection of targets on each of the noisy images as well as the noiseless reference set. Because the locations of the grains on each image are subject to statistical fluctuations, variations in shape and visibility occurred for the targets with low SNR. This meant that on the same image some targets of the same size were clearly visible while others were grossly misshapen or invisible. Large variations in the standard deviations were therefore expected in pointing to targets of the same size printed under similar conditions, as revealed in Figure 5. The typical range of observations is shown in Figure 6.

The observations on each target were made in seven sets of 15 observations with appropriate statistical tests being made for consistency within each set and between sets; a pooled standard deviation was derived from the seven sets. Standard deviations for the y-direction have been shown to be significantly larger than those of the x-direction by Roger and Mikhail (1969). However, while this appeared to be the case for several noiseless targets, there was not a consistent trend throughout, and therefore the x and y standard deviations were considered of equal weight when the interpolated lines were derived in Figures 5, 6 and 7.

DISCUSSION OF POINTING RESULTS

The standard deviations for *noiseless targets*, which have been presented in terms of *target annulus* in Figure 7, are larger than those obtained by O'Connor (1967) and Trinder (1971) (indicated by the broken line), especially for the smaller targets. This is primarily due to the lower measuring precision of the Wild A8 in comparison to the equipment which was used for the earlier experiments. For observer JCT, the only common observer in the two sets of data, the pattern is similar. However, for noisy samples for which there is a significant increase in standard deviation, the effect of this loss in precision should be marginal.

Standard deviations for *noisy targets* are presented against SNR, in Figure 5 for a target annulus of 2.3 mrad, while a summary is given for all annulus sizes in Figure 6. Horizontal lines for observations to targets at high SNR, i.e., equivalent to noiseless targets have been interpolated from Figure 7; the terminal point on each graph at low SNR indicates the approximate SNR at which the targets became impossible to locate. As there are substantial variations in the precisions derived for the noisy targets, some flexibility was necessary when the path of each line was plotted. However, because past experience has shown that in psychophysical studies there is a linear relation on logarithmic scales between stimuli and human performance, the lines shown in Figures 5 and 6 are justified (Stevens, 1962). Over these sections of the graphs, as the SNR is halved, the standard

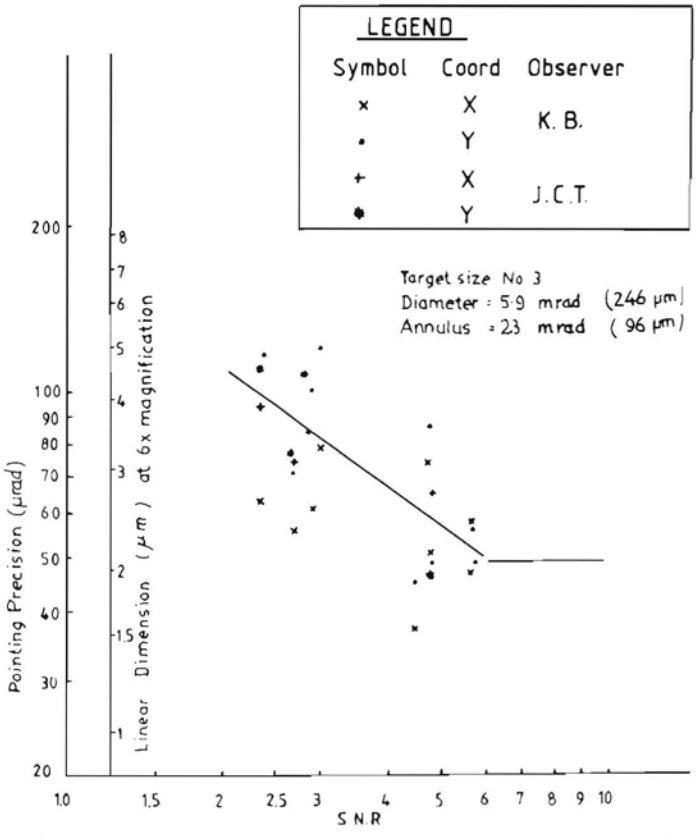

FIG. 5. Pointing precisions derived for noisy sharp targets with an annulus size of 2.3 mrad, plotted against SNR.

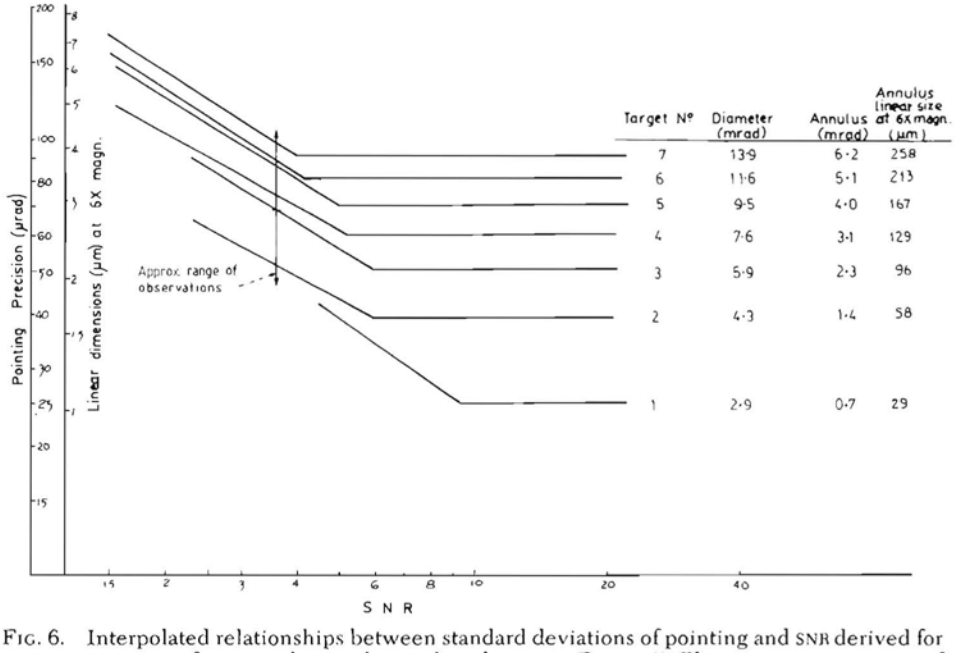

Target N°	Diameter (mrad)	Annulus (mrad)	Annulus linear size at 6x magn. (μm)
7	13·9	6·2	258
6	11·6	5·1	213
5	9·5	4·0	167
4	7·6	3·1	129
3	5·9	2·3	96
2	4·3	1·4	58
1	2·9	0·7	29

FIG. 6. Interpolated relationships between standard deviations of pointing and SNR derived for seven target sizes from graphs similar to that shown in Figure 5. The approximate range of standard deviations for each line is shown with reference to the graph for target size 3.

deviation of pointing increases by approximately 60 percent. This may occur, for example, if the RMS granularity of the photography were doubled by using different film or chemistry (Trinder, 1980). Threshold SNR, below which pointing precisions are affected by the noise in the image, decreases from about 9.5 for the small target annulus of 0.7 mrad to 4.0 for the large target annulus of 6.2 mrad, equal to 29 μm to 258 μm, respectively, at 6× magnification. It was found that the results of observations for targets with a ΔD of 0.7, but the same SNR were not significantly different from results obtained for targets with a ΔD of 0.3. A change in the background density of the targets also had no significant effect on results in Figure 6.

By interpolation from Figure 6, precisions of pointing for SNR's from 6 to 1.5 have been plotted in Figure 7 (with dotted lines) against annulus size. Noise increased the standard deviations of pointing from approximately 2 percent for noiseless targets to more than 3 percent for targets with a SNR of 1.5. The pattern of results shown in Figures 5 and 6 are similar to those derived in Trinder (1971) for blurred targets, where the parameter was slope of the density profile of the target. Noise and blur together, therefore, will result in an even greater loss in precision than that shown in Figure 7.

The expression of SNR in Equation 6 provides a simple yet easily determined quantity using parameters of density that are readily available. It also demonstrates a relationship in terms of total signal and noise power and hence may be considered to encompass the frequency spectrum, as discussed in the following section.

SPATIAL FREQUENCY DOMAIN

In Figure 3, the maximum values of the power spectra increase while the frequency ranges decrease as the targets become larger. The ratio of total power/noise power, equal to $(\text{SNR})^2$, is demonstrated by the ratio of areas under the corresponding curves. As noise is introduced into Figure 3 through the Wiener spectrum, there is a greater effect on the power spectrum curves of small targets, with a smaller enclosed area, than on the spectrum of large targets. By consequence, pointing precisions of small targets in Figure 6 are affected by noise at higher SNR's.

The noise and power spectra in Figure 3 can be studied to investigate the effects of magnification on observations to noisy targets. For a target size 3, 5.9 mrad in diameter, viewed at 6× magnification the power spectrum is shown in Curve 4, while the noise spectrum is also shown schematically as

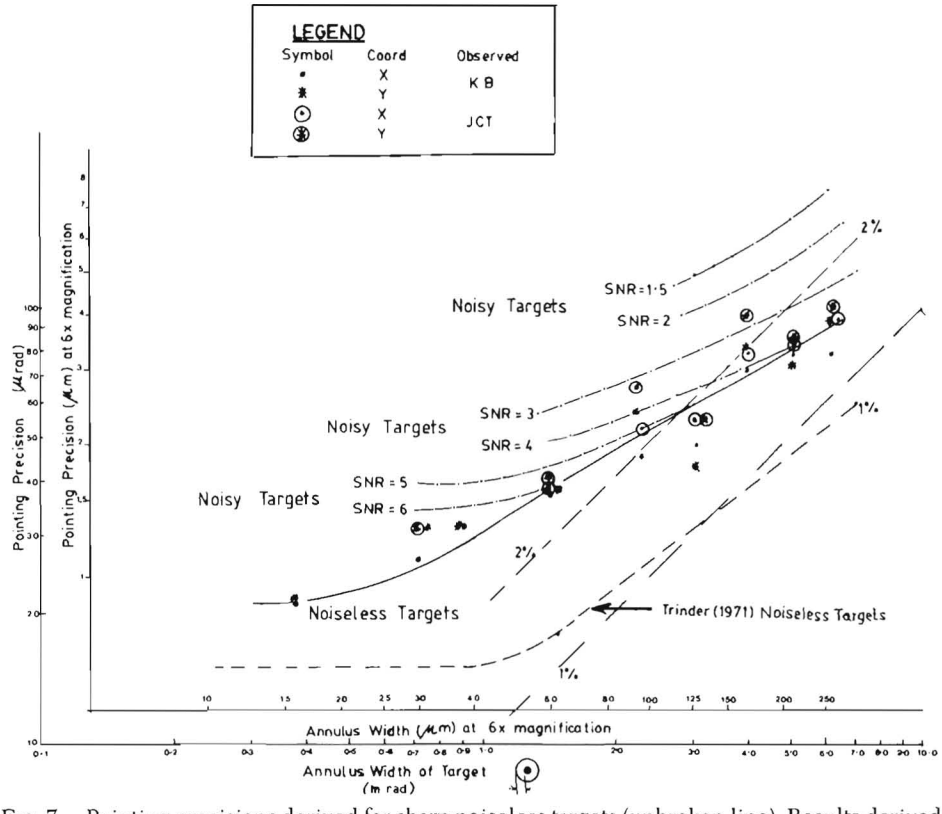

FIG. 7. Pointing precisions derived for sharp noiseless targets (unbroken line). Results derived in an earlier study (Trinder, 1971) are shown by broken line. Pointing precisions derived in this study for targets with SNR have been interpolated from Figure 6 and plotted by dotted lines.

Curve 1. If the magnification is increased to 12×, the power spectrum of the 11.8 mrad target now seen by the observer will be similar to Curve 7 while the noise power can be shown to remain substantially the same for many granularity samples, being derived with an aperture of 48 μm (2.4 mrad). The increase in magnification leads to an increase in the maximum power of the target together with a reduction in the frequency range. Noise power, though only having a small effect on low frequencies of the 11.8 mrad target, will limit the range of high spatial frequencies.

The efficiency of visual observations is presumably dependent on both the maximum value of the power spectrum, which apparently affects visibility, and the frequency range, which affects apparent sharpness. The choice of a suitable optical magnification during measurements to targets is a compromise between the desire to increase maximum power by increasing optical magnification and the consequent loss in sharpness (reduction in frequency range) of the target as the effects of noise become greater. To date, studies by Neville and Saunders (1974) and Welch and Lo (1977) have defined the optimum magnification required for viewing in terms of resolution rather than parameters of the power and noise spectrum. This paper highlights some interesting aspects of noise and power spectra of the targets in relation to optical magnification.

To examine further the effects of higher optical magnifications on observations to noisy sharp targets, pointing precisions for a target size of 118 μm and measuring mark size of 60 μm have been investigated. Kodak 2405 aerial film is assumed, for which RMS granularity at a density of 1.0 recorded with scanning aperture diameters of 96 μm, 48 μm, 24 μm, and 12 μm are 0.015*D*, 0.03*D*, 0.06*D*, and 0.12*D* (Trinder, 1980) for 6×, 12×, 24×, and 48× optical magnification, respectively. For two target contrasts of 0.3*D* and 0.7*D*, the SNR's and pointing precisions in μm derived from Figure 6 are shown in Table 1.

The improvement in pointing precision in Table 1 when the magnification is increased is only marginal, particularly for low contrast targets. Indeed, if the magnification is further increased, it can be shown that the pointing precisions will commence to deteriorate. Therefore, there is no advantage in increasing the magnification beyond about 24× for this example. For other display systems where SNR's are lower, the impact of higher magnifications will become even more significant.

Detection and Recognition

EARLIER RESEARCH

Welch and Halliday (1973) carried out studies on the detectability and measurability of photogrammetric signals under variable optical magnifications in which the effects of noise in the photography were not assessed. For detection and recognition, the minimum sizes of the objects were found to be 10 to 30 μm and 20 to 60 μm, which may be expressed as 1 to 2 times the width of the spread function of the photogrammetric system. Charman (1975, 1977), describing an extensive series of experiments on the resolution of repetitive targets and the detection and recognition of squares and circles on photographs, showed that the sizes of the square and circular targets required for recognition in these experiments were approximately 2 to 3 times the sizes of targets required for detection, both detection and recognition being a function of the reciprocal of the target size. Effects of noise in the photography were not determined by Charman, though its influence would have been apparent at high optical magnifications.

Barnard (1972) performed observations on noisy targets of the Landolt C, digits and Spokes-type (radiating line segments) targets under observation conditions similar to those used for photogrammetric and remote sensing observations. That is, unlimited viewing time was allowed and observers were permitted to vary the viewing magnification so that the angular subtense of the object suited them. Barnard also found a relationship existed between the reciprocal of the target size and the probability of detection. Further research is required, however, to determine the influence of noise on detection and recognition of objects associated with photogrammetry and remote sensing.

OBSERVATIONS

Circular, square, triangular, and diamond shaped targets with background noise were

TABLE 1

Magnification	Annulus Size Angul. Subt. mrad	Target Contrast 0.3D SNR	Target Contrast 0.3D Pointing Precision (μm)	Target Contrast 0.7D SNR	Target Contrast 0.7D Pointing Precision (μm)
6×	0.7	20	1	47	1
12×	1.4	10	0.8	23	0.8
24×	2.8	5	0.6	11	0.6
48×	5.6	2.5	0.6	5.5	0.5

printed with sizes ranging from 180 μm to 611 μm. In a Wild A8 with 6× magnification, the sizes were equivalent to angular subtenses from 4.3 to 14.7 mrad. These figures refer to the dimensions of the sides of squares, triangles, and diamonds, and the diameter of the circles. Simple shapes were considered initially but subsequent research should consider more complex figures. However, it is believed that the shapes studied are similar to images of man-made features requiring identification in remote sensing.

Thirteen separate images were printed with varying degrees of signal ΔD and RMS granularity. Typical examples of such images are shown in Figure 8. On each image there were five targets each of four sizes and four shapes, 80 targets in all. The positions of all objects were determined and stored in core in an on-line desk calculator. Each image was observed three times, giving a total of 15 observations on each shape and size; about 3,000 observations were made. Targets were observed systematically over the images. Successful detection was judged by the on-line desk calculator if the observer could correctly point with the measuring mark to a visible object in the image within 0.14 mm of the coordinates of any object held in the calculator (0.5 mm in model space of the Wild A8); otherwise, the pointing was considered to be an erroneous detection or false pointing. The task itself was not considered to be one of pointing but simply one of locating the approximate position of the feature. Having detected an object, the identification was checked against the correct identification stored in the calculator. Statistics for the total detection and recognition of each shape and size of target were assessed at the end of the observations on each image.

The percentage of correct responses in the observations for each target may be interpreted as a probability, provided the number of observations is sufficient to represent the overall population of observations. Fifteen observations on each target shape and size were considered insufficient to determine a reliable estimate of probabilities and, therefore, results were pooled by adding the total number of successful observations, first, for all target shapes for each size, and second, for all target sizes for each shape. Each value so derived was, therefore, based on 60 observations. The relationship between shape and target size was studied using the contingency coefficient (Dubois, 1965) based on the probabilities of detection and recognition for each target size and shape, and the pooled probabilities. By this method, the probabilities of recognition and detection for each target size appeared to be uncorrelated with those of each shape.

Results for target sizes of 7.3 mrad and 14.7 mrad (304 μm and 613 μm, respectively, at 6× magnification) have been plotted against SNR in Figure 9, while the summary for all four target sizes is given in Figure 10. A probability of 75 percent correct responses was used as a measure of detection and recognition of details and plotted against target size in Figure 11. The 75 percent probabilities of detection and recognition for targets of different shapes are given in Table 2.

DISCUSSION OF RESULTS OF DETECTION AND RECOGNITION

Consistent with the findings of Charman (1977) and Barnard (1972), the probabilities of detection and recognition are inversely proportional to target size, and directly proportional to the SNR of

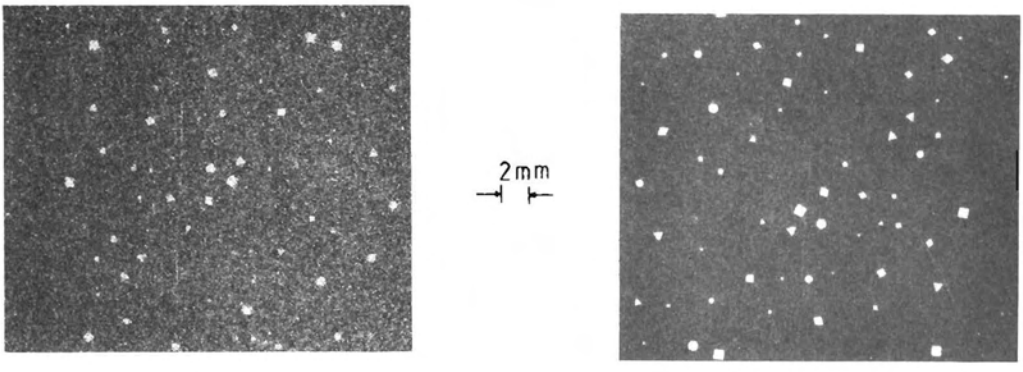

FIG. 8. Typical examples of noisy targets observed in detection and recognition tasks. Dimensions and SNR of the original samples are shown. Observations were made at an optical magnification of 6×.

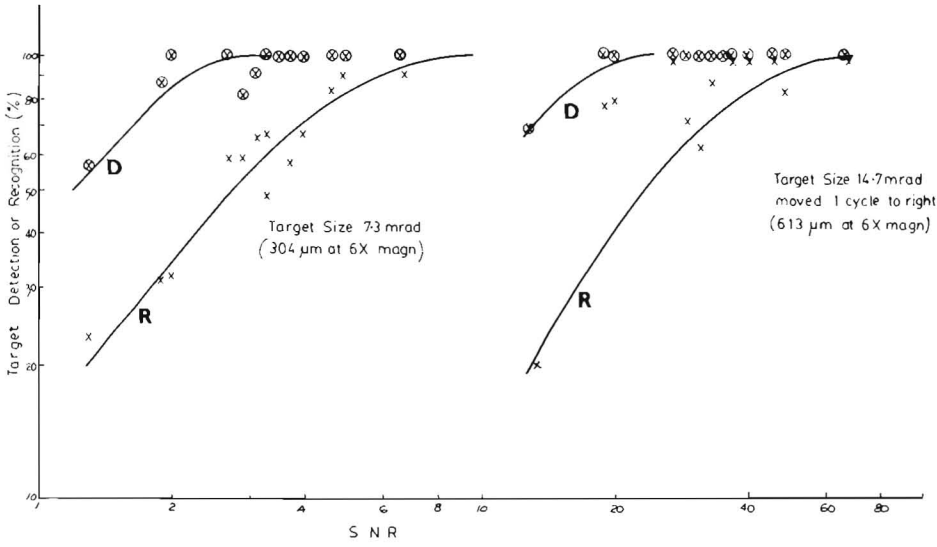

FIG. 9. Detection (D) and Recognition (R) for two sizes of targets for all shapes, expressed as the percentage of correct responses, in terms of SNR.

the target. Detection and recognition are unaffected by noise if the SNR is greater than about 2 to 3 and 6 to 7, respectively. Below these values, the probabilities of detection and recognition are approximately halved when the SNR is halved. The decline in the probabilities of success of these tasks for increasing noise (lower SNR) is similar to that shown by (Charman, 1977) for increasing blur in the image. The relationship between these two factors, however, is not known. In Figure 11, the relationship between target size and SNR for a 75 percent probability is non-linear, becoming asymptotic at SNR's of 3 and 1.5 for detection and recognition, respectively, as target sizes approach 20 mrad (0.8 mm at 6× optical magnification). Apparently, for target sizes greater than 20 mrad, detection and recognition will remain independent of target size for a given SNR.

While the geometric dimensions of the four objects were almost equal, the ratio of (target area/target area of triangle)$^{1/2}$, shown in Table 2, indicates that the differences in the minimum SNR for 75 percent probability of detection and recognition of squares, diamonds, and triangles is a func-

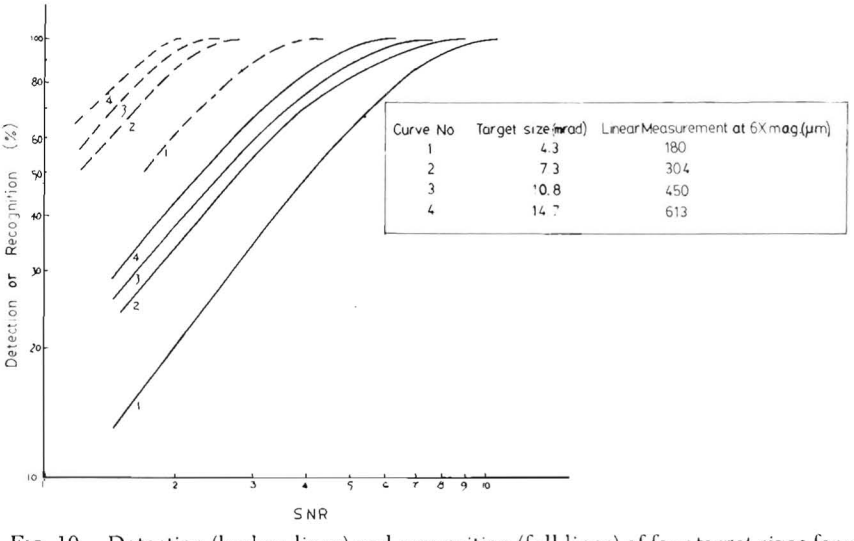

FIG. 10. Detection (broken lines) and recognition (full lines) of four target sizes for all shapes, expressed as the percentage of correct responses, in terms of SNR.

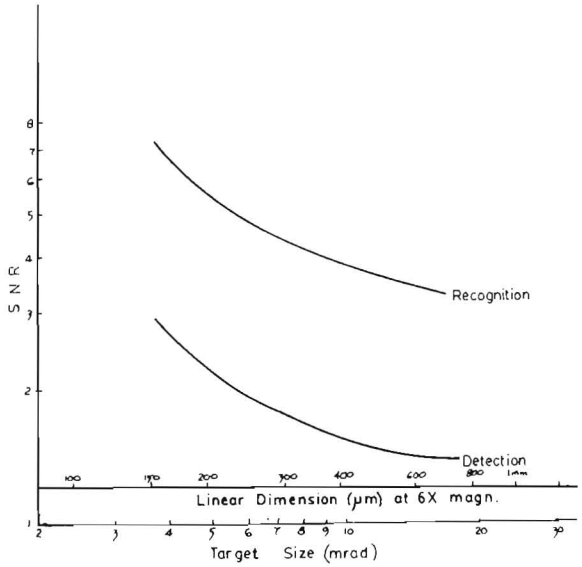

FIG. 11. Relationship between SNR and target size for a 75 percent probability of correct response.

tion of the areas of the objects and not of their actual shapes. Circular objects, however, result in a substantially worse performance than angular shaped targets.

The visual factors affecting detection and recognition in the presence of noise appear to be similar to those affecting these tasks when blurred targets are observed (Charman, 1977). As was concluded for pointing observations, if objects viewed are subject to both blur and noise produced by photographic grain, these aspects will combine in determining the effectiveness of these tasks. Effects of noise on the detection and recognition of more complex objects on displayed images used for either topographic mapping or remote sensing purposes have yet to be studied. Such features as man-made structures requiring identification or low contrast natural features requiring detection are typical examples.

CONCLUSIONS

- The signal-to-noise ratio was defined by the formula $\Delta D/\text{RMS}$, where ΔD represents the density difference of the target above background, and RMS granularity is determined with a circular scanning aperture diameter equivalent to 48 μm at 12× optical magnification. Scanning aperture diameters should follow an inverse linear relationship with respect to magnification if other magnifications are used.
- The maximum SNR at which pointing precisions are affected by noise varies from 9.5 for small target annuli of 0.7 mrad (29 μm at 6× magnification) to 4.0 for large target annulus sizes of 6.2 mrad (258 μm at 6× magnification). For SNR's lower than these figures, pointing precision will increase by approximately 60 percent when the SNR is halved.
- It has been shown that in practice as optical magnification is increased the SNR will decrease and, therefore, noise will have a greater effect on the pointing precisions of observations. There is, therefore, no advantage in increasing the optical magnification beyond a particular value which is dependent on the SNR of the image being viewed.
- The probability of detection of geometric objects is reduced by noise when the SNR drops below 4 for small objects of 4.3 mrad (180 μm at 6× magnification) or to 2 for large targets of 14.7 mrad (613 μm at 6× magnification). Below these levels the probability of detection is approximately halved as the SNR is also halved. Recognition of objects is achieved at SNR's 2 to 3 times those for detection. Angular objects are more easily detected and recognized than circular objects.

ACKNOWLEDGMENTS

This research has been supported by a Grant from the Australian Research Grants Committee. The work of Mr. Ken Bullock in carrying out the observations is also acknowledged.

REFERENCES

Barnard, T. W., 1972. Image evaluation by means of target recognition. *Phot. Sci. Eng.* Vol. 16, pp. 144-150.

Biberman, L. M., 1973. *Perception of Displayed Information.* Plenum Press, New York.

Charman, W. N., 1975. Visual Factors in Photographic Detection, Recognition and Resolution Tasks. Part I—Resolution. *Phot. Sci. Eng.* Vol. 19, pp. 228-234.

———, 1977. Visual Factors in Photographic Detection, Recognition and Resolution Tasks. Part II—Detection and Recognition. *Phot. Sci. Eng.* Vol. 21, pp. 204-208.

Charman, W. N., and A. Olin, 1965. Tutorial. Image

TABLE 2

	MINIMUM SNR for 75% probability of detection	MINIMUM SNR for 75% probability for recognition	(Target Area/ Area of Triangle)$^{1/2}$
Circular	2.8	5.1	1.3
Triangle	2.4	4.5	1.0
Diamond	2.0	4.1	1.2
Square	1.3	3.6	1.5

Quality Criteria for Aerial Camera Systems. *J. Phot. Sci. Eng.* Vol. 9, pp. 385-397.

Dubois, P. H., 1965. *An Introduction to Psychological Studies*. Harper & Row—John Weatherill, New York.

Halmshaw, R., 1971. The Influence of Film Granularity on Image Detail on Radiographs. *J. Phot. Sci.* Vol. 19, pp. 167-177.

Hempenius, 1964. Aspects of Photographic Systems Engineering. *Applied Optics* 3, pp. 45-53.

Hufnagel, R. E., 1965. "The Practical Application of Modulation Transfer Functions." Unpublished paper of Symposium held by Soc. Photo. Sci. and Engng. reported by Biberman (1973).

James, T. H. (ed.), 1977. *The Theory of the Photographic Process*. McMillan Publishing Co. Inc.

Neville, R. S., and A. E. Saunders, 1974. Resolving Power/Exposure Relation for Black-and-White Emulsion Layers. *J. Photo. Sci.* Vol. 22, pp. 181-186.

O'Connor, D. C., 1967. *Visual Factors Affecting the Precision of Coordinate Measurements in Aerotriangulation*. University of Illinois, Photogrammetry Series, No. 6.

Roger, R. E., and E. M. Mikhail, 1969. *Study of the Effects of Non-homogeneous Target Backgrounds on Photogrammetric Measurements*. Research Report, Purdue University, W. Lafayette, Indiana, U.S.A.

Scott, F., 1968. The Search for a Summary Measure of Image Quality—A Progress Report. *Phot. Sci. Eng.* Vol. 12, pp. 154-164.

Stevens, S. S., 1962. The Surprising Simplicity of Sensory Matrices. *American Psychologist*, Vol. 17, pp. 29-39.

Stultz, K. F., and H. J. Zweig, 1959. Relationship between Graininess and Granularity for Black-and-White Samples with Non-uniform Granularity Spectra. *J. Opt. Soc. Am.*, Vol. 49, pp. 693-702.

Trinder, J. C., 1971. Pointing Accuracies to Blurred Signals. *Photo. Engng.* Vol. 37, pp. 192-202.

———, 1980. Aerial Film Granularity and Its Influence on Visual Performance. *Proceedings International Society for Photogrammetry Congress*, Hamburg, 1980. Vol. 23, No. 1, pp. 167-181.

Welch, R., and J. Halliday, 1973. Imaging Characteristics of Photogrammetric Camera Systems. *Photogrammetria*, Vol. 29, pp. 1-43.

Welch, R., and C. P. Lo, 1977. Height Measurements from Satellite Images. *Photo. Engng. & Remote Sensing* Vol. 43, pp. 1233-1241.

Zwick, D. M., 1965. "Film graininess and density—A critical relationship." *Phot. Sci. Engng.* Vol. 16, pp. 345-348.

Zwick, D. M., and D. L. Brothers, Jr., 1975. RMS Granularity: Determination of Just-Noticeable Differences. *Phot. Sci. Engng.* Vol. 19, pp. 235-238.

(Received 5 June 1981; revised and accepted 19 March 1982)

Forthcoming Articles

O. O. Ayeni, Phototriangulation: A Review and Bibliography.

O. O. Ayeni, Optimum Sampling for Digital Terrain Models: A Trend Towards Automation.

R. G. Best, R. Fowler, D. Hause, and *M. Wehde*, Aerial Thermal Infrared Census of Canada Geese in South Dakota.

P. D. Carman, Aerial Camera Vibration.

David O. Cook, Gary R. Davis, Ronald A. Franklin, and *Timothy L. Flynn*, Use of Aerial Photography with Loran C Positioning to Map Offshore Surface Currents.

Richard L. Deuell and *Thomas M. Lillesand*, An Aerial Photographic Procedure for Estimating Recreational Boating Use on Inland Lakes.

Thomas L. Erb and *Warren R. Philipson*, Producing Stereo Teaching Aids from Aerial Photographs.

Barry M. Evans, Aerial Photographic Analysis of Septic System Performance.

R. D. Graetz and *M. R. Gentle*, The Relationships between Reflectance in the Landsat Wavebands and the Composition of an Australian Semi-Arid Shrub Rangeland.

Charlotte M. Gurney and *John R. G. Townshend*, The Use of Contextual Information in the Classification of Remotely Sensed Data.

M. A. Hardisky, V. Klemas, and *R. M. Smart*, The Spectral Radiance of Spartina alterniflora Canopies.

J. L. Heilman and *D. G. Moore*, Evaluating Depth to Shallow Groundwater Using Heat Capacity Mapping Mission (HCMM) Data.

John R. Jensen and *Michael Hodgson*, Remote Sensing Brightness Maps.

L. Daniel Maxim and *Leigh Harrington*, To Mix or Match: On Choosing Matched Samples in Comparative Aerial Surveys.

A. Prieto, J. Bescós, and *J. Santamaría*, Spatial Frequency Pseudocolor Filters.

Manmohan M. Trivedi, Clair L. Wyatt, and *David R. Anderson*, A Multispectral Approach to Remote Detection of Deer.

Kam W. Wong and *Youssuf Mustafa Siyam*, Accuracy of Earthwork Calculations from Digital Elevation Data.

Daniel K. Zigich and *Kenneth E. Kolm*, Evaluating the Effectiveness of Landsat Data as a Tool for Locating Buried Pre-Glacial Valleys in Eastern South Dakota.